



THE UNIVERSITY *of* EDINBURGH

Edinburgh Research Explorer

Drug 'clicking' on cell-penetrating fluorescent nanoparticles for in cellulo chemical proteomics

Citation for published version:

Valero, T, Delgado-gonzález, A, Unciti-broceta, JD, Cano-cortés, V, Pérez-lópez, A, Unciti-broceta, A & Sánchez-martín, R 2018, 'Drug 'clicking' on cell-penetrating fluorescent nanoparticles for in cellulo chemical proteomics', *Bioconjugate chemistry*, vol. 29, no. 9, pp. 3154–3160.
<https://doi.org/10.1021/acs.bioconjchem.8b00481>

Digital Object Identifier (DOI):

[10.1021/acs.bioconjchem.8b00481](https://doi.org/10.1021/acs.bioconjchem.8b00481)

Link:

[Link to publication record in Edinburgh Research Explorer](#)

Document Version:

Peer reviewed version

Published In:

Bioconjugate chemistry

General rights

Copyright for the publications made accessible via the Edinburgh Research Explorer is retained by the author(s) and / or other copyright owners and it is a condition of accessing these publications that users recognise and abide by the legal requirements associated with these rights.

Take down policy

The University of Edinburgh has made every reasonable effort to ensure that Edinburgh Research Explorer content complies with UK legislation. If you believe that the public display of this file breaches copyright please contact openaccess@ed.ac.uk providing details, and we will remove access to the work immediately and investigate your claim.



Drug ‘clicking’ on cell-penetrating fluorescent nanoparticles for in cellulo chemical proteomics

Teresa Valero, Antonio Delgado-González, Juan Diego Unciti-Broceta, Victoria Cano-Cortés, Ana Pérez-López, Asier Unciti-Broceta, and Rosario Sánchez-Martín

Bioconjugate Chem., **Just Accepted Manuscript** • DOI: 10.1021/acs.bioconjchem.8b00481 • Publication Date (Web): 18 Aug 2018

Downloaded from <http://pubs.acs.org> on August 20, 2018

Just Accepted

“Just Accepted” manuscripts have been peer-reviewed and accepted for publication. They are posted online prior to technical editing, formatting for publication and author proofing. The American Chemical Society provides “Just Accepted” as a service to the research community to expedite the dissemination of scientific material as soon as possible after acceptance. “Just Accepted” manuscripts appear in full in PDF format accompanied by an HTML abstract. “Just Accepted” manuscripts have been fully peer reviewed, but should not be considered the official version of record. They are citable by the Digital Object Identifier (DOI®). “Just Accepted” is an optional service offered to authors. Therefore, the “Just Accepted” Web site may not include all articles that will be published in the journal. After a manuscript is technically edited and formatted, it will be removed from the “Just Accepted” Web site and published as an ASAP article. Note that technical editing may introduce minor changes to the manuscript text and/or graphics which could affect content, and all legal disclaimers and ethical guidelines that apply to the journal pertain. ACS cannot be held responsible for errors or consequences arising from the use of information contained in these “Just Accepted” manuscripts.



Drug 'clicking' on cell-penetrating fluorescent nanoparticles for *in cellulo* chemical proteomics

Teresa Valero^{†,‡}, Antonio Delgado-González[‡], Juan Diego Unciti-Broceta^{‡,‡}, Victoria Cano-Cortés[‡], Ana M. Pérez-López[†], Asier Unciti-Broceta^{†,*} and Rosario M. Sánchez Martín^{‡,*}

[†] Cancer Research UK Edinburgh Centre, MRC Institute of Genetics & Molecular Medicine, University of Edinburgh, Edinburgh EH4 2XR, UK.

[‡] GENYO, Centre for Genomics and Oncological Research: Pfizer / University of Granada / Andalusian Regional Government, PTS Granada -Avda. Ilustración 114- 18016 Granada, Spain.

[‡]Nanogetics SL, Avenida de la Innovación 1, Parque Tecnológico Ciencias de la Salud, Edificio BIC, 18100 Armilla, Granada, Spain.

KEYWORDS. *Drug-polymer conjugate, click chemistry, CuAAC, target ID, Baeyer test, cell-penetrating nanoparticles.*

ABSTRACT: Chemical proteomics approaches are widely used to identify molecular targets of existing or novel drugs. This manuscript describes the development of a straightforward approach to conjugate azide-labelled drugs *via* click chemistry to alkyne-tagged cell-penetrating fluorescent nanoparticles as a novel tool to study target engagement and/or identification inside living cells. A modification of the Baeyer test for alkynes allows monitoring the Cu(I)-catalyzed azide-alkyne cycloaddition (CuAAC) reaction, guaranteeing the presence of the drug on the solid support. As a proof of concept, the conjugation of the promiscuous kinase inhibitor dasatinib to Cy5-labelled nanoparticles is presented. Dasatinib-decorated fluorescent nanoparticles efficiently inhibited its protein target SRC *in vitro*, entered cancer cells and colocalized with SRC *in cellulo*.

INTRODUCTION

Drug discovery efforts across industry and academia has generated extensive libraries of small molecule compounds that are recurrently used in high-throughput screening campaigns. One of such tests employs cell assays to search for compounds that elicit phenotypic responses in particular disease models in a target agnostic manner. This approach, so-called phenotypic screening, is aimed to accelerate the earlier stages of drug discovery and, potentially, favor the finding of first-in-class inhibitors¹⁻³. After a phenotypic hit or lead is found, one of the main challenges is to elucidate the mechanism of action responsible for the observed pharmacological effect,⁴ as the assays only provide information on compounds' activity in the cell model of choice without informing on the target.⁵ Consequently, target identification (ID) studies are often performed to support subsequent lead optimization campaigns.

Among the strategies developed for target ID, chemical proteomics enable to interrogate the full proteome for direct drug-target interactions. Most chemical proteomics approaches combine affinity chromatography with advanced mass spectrometry to enrich and facilitate target identification from complex biological samples⁶. An alternative approach has been proposed to directly visualize drug-target interactions in cells using drug-labelled nanodevices and fluorescent immunocytochemistry⁷. Regardless of the method, an essential step in these strategies is the conjugation of the drug to the solid support, which typically requires individual optimization of the coupling process for each drug⁸. Therefore, the development of versatile, robust conjugation methods are essential to

facilitate the performance of target ID studies both in cell lysates and in native biological environments.

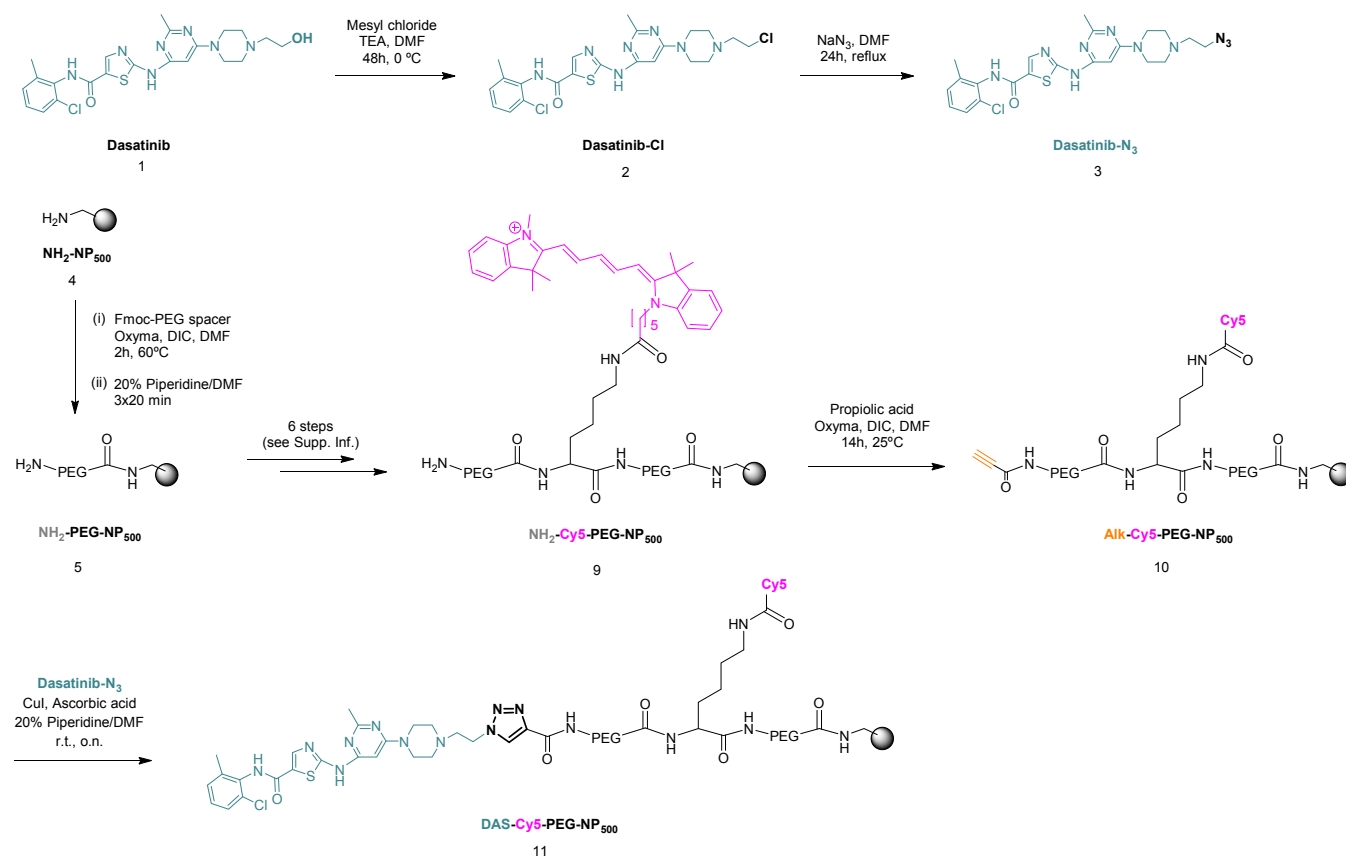
Herein, we present a straightforward procedure for the conjugation of azide-tagged drugs to miniaturized solid supports by click chemistry, along with an analytical method to rapidly determine whether the coupling reaction has been successful. As a proof of concept of the strategy, the synthesis, characterization and biological validation – *in vitro* and *in cellulo* – of a novel cell-penetrating fluorescent nanodevice decorated with the tyrosine kinase inhibitor (TKI) dasatinib is reported.

RESULTS AND DISCUSSION

Selection and Development of Azide-Tagged Dasatinib.

Dasatinib is a potent promiscuous kinase inhibitor approved by the FDA for the treatment of chronic myeloid leukaemia (CML) after acquired resistance to imatinib⁹. Dasatinib's therapeutic effect is mediated by inhibition of the constitutively-active fusion protein BCR-ABL, which is the product of an aberrant chromosomal translocation and responsible for CML oncogenesis. Nevertheless, dasatinib also inhibits a wide range of kinases including the nonreceptor tyrosine kinase SRC and its family members (LCK, HCK, YES, FYN, FGR, BLK, LYN, FRK), receptor tyrosine kinases (KIT, PDGFR, DDR1/2, c-FMS, ephrin receptors), and TEC family kinases (TEC and BTK)¹⁰, representing a good example of a promiscuous drug with potential use against numerous clinical disorders. The high potency of dasatinib, its interesting polypharmacological properties and its easy-to-functionalize chemical structure made it an optimal candidate to develop and test our strategy.

Scheme 1. Synthesis of dasatinib-decorated fluorescently-labelled cell-penetrating nanoparticles.



To introduce an azide “handle” in dasatinib for CuAAC reactions while retaining the essential kinase binding elements of its structure, the terminal hydroxyl group of the hydroxyethylpiperazinyl moiety was modified. The role of this moiety is to impart water solubility to the compound⁷ and it is displayed outside the protein in the SRC-dasatinib co-crystal structure¹¹. The substitution of the OH of dasatinib by N₃ was efficiently carried out using a reported procedure with minor modifications^{7,12}. Briefly, chlorination of that position was achieved by treating dasatinib with mesyl chloride and trimethylamine. The corresponding chloro derivative **dasatinib-Cl (2)** was then reacted with sodium azide to obtain derivative **dasatinib-N₃ (3)** (Scheme 1, see full synthetic details in the Supp. Inf.). Cell viability assays against breast cancer MDA-MB-231 cells demonstrated that **3** retained the anti-proliferative properties of the parent drug **1** (see Supp. Inf.).

Synthesis of dasatinib-decorated Cy5-labelled cell-penetrating nanospheres. *In cellulo* chemical proteomics has the potential to provide more biologically relevant results by studying drug-target interactions in the native cellular environment¹³. It also provides a method to study target engagement, a relevant validation step in drug discovery programs. The development of facile and reliable strategies to conjugate drugs and fluorescent labels on devices with the capacity to penetrate cells without inducing toxicity is very attractive in this field. 500nm cross-linked polystyrene nanospheres with demonstrated capacity to safely penetrate a wide variety of cell types^{14–19} were redesigned for the goals of this project (Scheme 1). **NH₂-**

NP₅₀₀ (4) were synthesized and functionalized according to previous reports^{17,20}. To increase biocompatibility, prevent unspecific protein binding and maximize the freedom of the conjugated drug molecules, **4** were PEGylated before and after incorporation of the dye. By sequential coupling and orthogonal deprotection steps (Fmoc/Dde deprotection strategy²¹), bifunctionalized doubly-PEGylated nanoparticles (NPs) were labeled with the far-red fluorescent dye Cy5 (**NH₂-Cy5-PEG-NP₅₀₀, 9**). Then an alkyne handle was incorporated onto the NPs by conjugation of propionic acid²² to generate **Alk-Cy5-PEG-NP₅₀₀ (10)**. Finally, reaction of **10** and **3** in the presence of CuI and ascorbic acid²³ gave rise to dasatinib-decorated Cy5-tagged nanospheres, **DAS-Cy5-PEG-NP₅₀₀ (11)** (see synthesis and loadings in the Supp. Inf.). Number of NPs per unit of volume was calculated by spectrophotometry according to previous reports²⁴ (see calculations in the Supp. Inf.).

Analytical determination of dasatinib incorporation onto the solid support. Although CuAAC reactions are typically described as virtually quantitative even under mild conditions^{25,26}, click reactions on solid phase typically need optimized conditions to reach these standards^{27,28}. To confirm the effective coupling of **3** to the alkyne-tagged NPs **10**, a series of analytical methods were attempted: (i) detection of unreacted alkynes on the solid support by modification of the Baeyer test for alkynes; (ii) Zeta potential characterization of NPs at different steps of the synthesis; (iii) validation by NMR and mass spectrometry of the functionalization strategy by solid phase synthesis using an amino-functionalized resin (Rink amide resin).

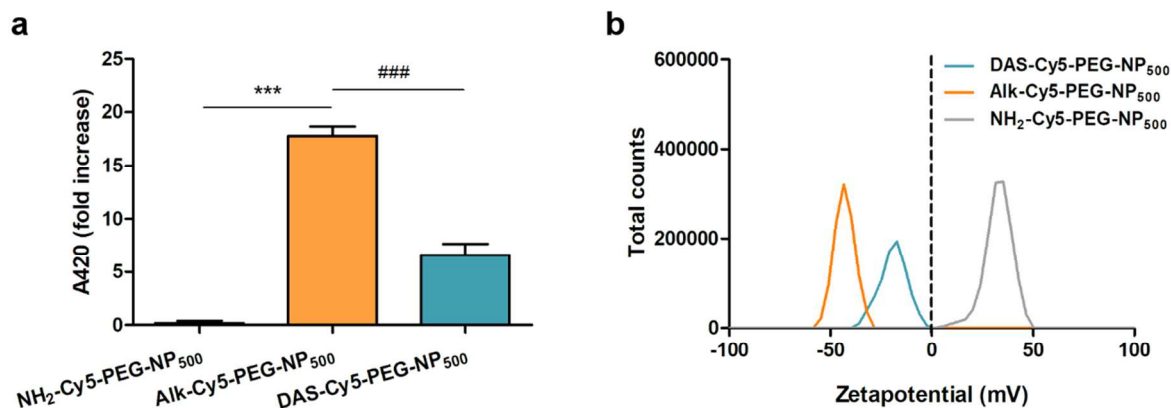


Figure 1. (a) Modification of the Baeyer test for alkynes detects the presence of unreacted alkynes on the NP surface. After reaction of each NP type with KMnO_4 , supernatants were analyzed for absorbance in a Nanodrop 3000 at 420nm. Data are means of fold increase related to KMnO_4 absorbance. Error bar = \pm SEM; $n=3$. (b) Zeta potential distribution of each NP type analyzed by a ZetaSizer Nano ZS.

The Baeyer test is routinely used in chemistry labs to detect the presence of double or triple carbon-carbon bonds based on the capacity of KMnO_4 to oxidize alkenes and alkynes. Aqueous reduction of KMnO_4 produces MnO_2 (blackish / brown color), a change that is detectable by spectrophotometry in the range of 250 to 500 nm^{24} . Therefore, we anticipated that this method could be used to detect unreacted alkynes on the NPs and thereby assess the efficacy of the drug incorporation reaction onto the solid support. **DAS-Cy5-PEG-NP₅₀₀ (11)** were treated with an aqueous solution of KMnO_4 and absorbance spectra analyzed, with the test of **NH₂-Cy5-PEG-NP₅₀₀ (9)** and **Alk-Cy5-PEG-NP₅₀₀ (10)** under the same conditions being used as negative and positive controls, respectively (see full details in the Suppl. Inf.). After exploring different reaction conditions and careful spectroscopic analysis to improve the method, the measurement of the changes in the absorbance values at 420 nm after 5 min reaction in comparison to the unreacted KMnO_4 solution was found to be optimal. As shown in Figure 1a, analysis of the reaction of the positive control **Alk-Cy5-PEG-NP₅₀₀** resulted in a significant increment of absorbance at 420 nm, a change that was undetectable for **NH₂-Cy5-PEG-NP₅₀₀** (which do not contain triple bonds). Importantly, the intensity of the signal was significantly reduced in **DAS-Cy5-PEG-NP₅₀₀**, as it would be expected after conjugation with **3** by CuAAC. This simple analytical test served to verify that the click reaction took place at a relatively high yield, yet some unreacted alkynes were still present in the structure of **DAS-Cy5-PEG-NP₅₀₀**, most probably being those less-accessible alkynes found in the interior of the polymeric framework of the NPs. An estimation of the CuAAC reaction yield can be performed with this spectrophotometric method, giving a value of 63.6%. Unreacted alkynes are likely to be found in the interior of the NPs, as steric constraints may affect the reaction efficacy.

Chemical moieties displayed at the outer layer of NPs influence the surface charge and consequently the Zeta potential of these colloidal structures²⁹. To further validate the results obtained from the Baeyer test, the conjugation of dasatinib to the NPs was also assessed by measuring

Zeta potential of **NH₂-Cy5-PEG-NP₅₀₀**, **Alk-Cy5-PEG-NP₅₀₀** and **DAS-Cy5-PEG-NP₅₀₀**. Figure 1b shows a displacement of Zeta potential distribution to the negative range when amines were substituted by alkynes, whereas upon drug conjugation the presence of the drug on the NP displaces the Zeta potential to less negative values, providing further qualitative evidence of the success of the CuAAC reaction.

As a final proof, rink amide resins (**NH₂-RINK**, typically used in solid phase peptide synthesis) were treated with **3** using the same reaction conditions used for the functionalization of the NPs (see Scheme 1). Following release of the corresponding triazolo-modified dasatinib derivate from the solid support by linker cleavage in acidic conditions, NMR analysis confirmed the efficacy of this conjugation reaction (see Suppl. Inf.).

Biological assays. To assess if the biological activity of the drug is maintained after conjugation onto the NPs, **DAS-Cy5-PEG-NP₅₀₀** were incubated with recombinant SRC and the activity of the kinase analyzed using a luminescence commercial kit. NPs without dasatinib (**NH₂-Cy5-PEG-NP₅₀₀**) were used as negative control. As shown in Figure 2a, a concentration dependent reduction in SRC activity was observed in the presence of **DAS-Cy5-PEG-NP₅₀₀**, with a 50% of inhibition observed at $2,041 \times 10^6$ NPs (51×10^3 NP / μL). By calculating the amount of drug per NP, the IC_{50} value was estimated to be 33.4 nM.

Crosslinked polystyrene NPs have been previously shown to rapidly enter a wide range of cell types^{14-19,30}. To prove that the presence of dasatinib does not interfere with the internalization process, cell uptake into MDA-MB-231 cells was analyzed by flow cytometry (Figure 2b and Suppl. Inf.) and time-lapse imaging (Movie S1). Cells exhibiting fluorescence in the Cy5 channel were considered as “nanofected” and multiplicity of nanofection 50 (MNF50) values were calculated as the ratio of nanoparticles per cell necessary to “nanofect” 50% of the cell population²⁴. As shown in Figure 2b, MNF50 values of **DAS-Cy5-PEG-NP₅₀₀** only were slightly inferior when compared to the unclicked control **NH₂-Cy5-PEG-NP₅₀₀**, although no differences in internalization efficiency were observed at ≥ 300 NPs/cell.

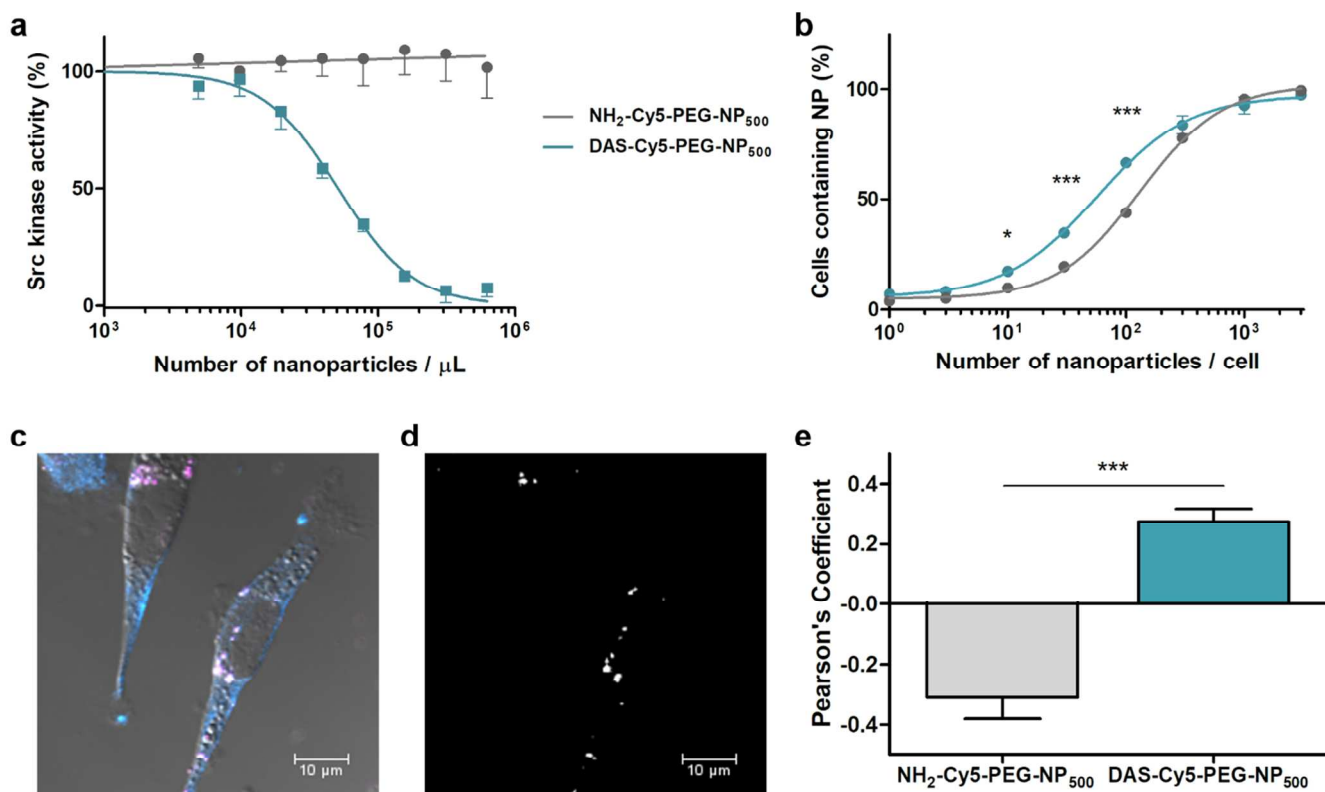


Figure 2. (a) Dasatinib-decorated NPs inhibit SRC kinase activity in a dose-dependent manner as measured by ADP Glo luminescent kinase assay. (b) Study of cellular uptake. MDA-MB-231 cells were incubated with concentrations ranging from 3 to 3000 **DAS-Cy5-PEG-NP₅₀₀** or **NH₂-Cy5-PEG-NP₅₀₀** per cell for 18 h and analyzed by flow cytometry. Dasatinib-decorated nanoparticles by MDA-MB-231 cells shows equivalent efficiency than for the control NPs at ≥ 300 NPs/cell. (c) Representative example of **DAS-Cy5-PEG-NP₅₀₀** internalized by MDA-MB-231 cells, Z-stack section imaged by confocal microscopy and zoomed. MDA-MB-231 cells were incubated with 3000 **NH₂-Cy5-PEG-NP₅₀₀** or **DAS-Cy5-PEG-NP₅₀₀** per cell (magenta) for 24 h, processed for immunocytochemistry and stained with anti-SRC primary and Dylight 405 secondary antibodies (cyan to white). (d) **DAS-Cy5-PEG-NP₅₀₀** colocalize with SRC kinase. Mask image of (c) facilitates visualization of colocalization pixels (in white). (e) Pearson's correlation coefficient was obtained with ZEN black software from images at zoom factor 1x and subjected to unpaired t-test with GraphPad Prism. Data are mean \pm SEM of duplicates of four independent experiments, *** $P < 0.001$.

Target engagement study. To test the functionality of the nanodevices in cells, we next performed a target engagement assay. Triple negative breast cancer MDA-MB-231 cells were selected to this study as SRC protein is highly overexpressed in these cells³¹. MDA-MB-231 cells were treated with **DAS-Cy5-PEG-NP₅₀₀** for 24 h and target-NP localization studied by confocal microscopy. The presence of a Cy5 fluorescent moiety on the NPs along with their size (500 nm) enabled the visualization of NPs by confocal microscopy into living cells. Immunocytochemistry analysis was carried out to visualize the SRC protein in the cells using an anti-SRC primary antibody and a fluorescent secondary antibody (Dylight 405). Z-stack images were acquired to image the NPs distributed throughout the cytoplasm (Figure 2c,d). Upon immunocytochemistry, image analysis showed co-localization of **DAS-Cy5-PEG-NP₅₀₀** with SRC protein in MDA-MB-231 cells. In contrast, the control NPs not decorated with dasatinib (**NH₂-Cy5-PEG-NP₅₀₀**) showed no colocalization with the target (see Supp. Inf.). These results were further confirmed by calculation of the Pearson's correlation coefficient (Figure 2e), demonstrating linear correlation (positive value) between

the localization of **DAS-Cy5-PEG-NP₅₀₀** and SRC. In contrast, a negative value was obtained by analysis the localization of **NH₂-Cy5-PEG-NP₅₀₀** and SRC. These results prove the capacity of **DAS-Cy5-PEG-NP₅₀₀** to efficiently engage with a specific target *in cellulo*.

CONCLUSIONS

In conclusion, herein we have presented a novel drug-decorated nanoprobe with the capacity to penetrate mammalian cells and bind target proteins in the intracellular environment. The use of a conjugation strategy based on the efficient CuAAC reaction makes this approach accessible to many different drugs by simple incorporation of an azide handle. Caution, however, should be taken when assuming a quantitative yield for click reactions on miniaturized devices. To avoid false negatives, a rapid spectrophotometric test for click reactions on alkyne-tagged solid supports was developed based on the Baeyer test. This method can be used to estimate the yield of coupling reaction by detecting unreacted alkynes on the solid support. As a proof of concept, fluorescent NPs were functionalized with dasatinib and the incorporation of the drug confirmed by different analytical methods. Dasatinib-decorated NPs

induced a reduction in SRC activity *in vitro*, further demonstrating drug incorporation on the solid support, but also proving a correct spatial arrangement of the conjugate that maintained drug bioactivity. These NPs were efficiently internalized into living MDA-MB-231 cells and, furthermore, demonstrated binding to the target protein (SRC kinase) *in cellulo*, proving the capacity of this novel nanodevice to detect drug-target interactions in complex living environments. The size of the nanoprobe (~500 nm in \varnothing) was selected based on the technical limitations of conventional fluorescence microscopy.³² Nevertheless, if high-resolution imaging techniques are available, the versatile methodology presented herein could be readily implemented on NPs of smaller size.³³

MATERIALS AND METHODS

General chemistry protocols. All commercially available chemicals were obtained from either Fisher Scientific, Matrix Scientific, Sigma-Aldrich or VWR International Ltd. Reactions were performed under inert atmosphere (nitrogen) using anhydrous solvents. NMR spectra were recorded at ambient temperature on a 500 MHz Bruker Avance III spectrometer. Samples were dissolved in deuterated solvents commercially available from Sigma-Aldrich. ¹H NMR spectra: chemical shifts are reported in parts per million (ppm) relative to tetramethylsilane. The data is presented as follows: chemical shift, integration, multiplicity (s = singlet, d = doublet, t = triplet, q = quartet, m = multiplet), coupling constants as a J value in Hertz (Hz) and interpretation. The number of protons (n) for a given resonance is indicated as nH, and is based on spectral integration values. The data is presented as follows: chemical shift and assignment. TLCs were ran on Merck TLC Silica gel 60 F254 plates, typically 5 cm x 10 cm, and monitored using a 254 nm UV source. High resolution mass spectra were recorded by the MS Department of the University of Edinburgh on a Thermo MAT 900 XLP high resolution, double focussing mass spectrometer. All the couplings were carried out on the Eppendorf Thermomixer® comfort and washed after centrifugation in an Eppendorf mini centrifuge.

Conjugation of dasatinib to NPs. **8** (1 mL; 1 eq) were suspended in DMF (1 mL). Separately, propiolic acid (50 eq) was dissolved in DMF and activated by the addition of oxyma (50 eq) for 4 minutes at r.t. before the addition of DIC (50 eq; Sigma-Aldrich) and mixed for 8-10 minutes at r.t. The solution mixture was then added to nanospheres and suspension mixed on the Thermomixer at 1400 rpm for 14 hours at 25°C to obtain alkyne-functionalized nanospheres **10** after centrifugation and subsequently washing with DMF (3 x 1 mL) MeOH (3 x 1 mL), deionized water (3 x 1 mL). 500 μ L of **10** were washed, suspended in DMF and centrifuged. Separately, a mixture of DMF: piperidine (4:1) was degassed and a solution of CuI (30 eq), ascorbic acid (60 eq), **3** (30 eq) in 500 μ L degassed DMF: piperidine (4:1) under nitrogen bubbling. This mixture was added onto resins while bubbling nitrogen, sealed and mixed overnight in a rotary wheel. Dasatinib-labelled nanospheres, **11** were obtained by centrifugation and subsequently washed with DMF (3 x 500 μ L), MeOH (3 x 500 μ L), deionized water (3 x 500 μ L).

Baeyer test for alkynes. 1 μ L of stock KMnO₄ solution (2.5 mM) was added to 5 x 10⁸ NPs or 0.5 mg rink amide resins to a final volume of 10 μ L in water. NPs and resins were then centrifuged at 13000 g for 5 minutes in an Eppendorf centrifuge and absorbance spectra were analyzed. 420 nm absorbance was represented as fold increase to control solution of KMnO₄.

Dynamic Light Scattering and Zeta potential. The hydrodynamic size and Zeta potential of intermediate and final nanoparticle configurations were measured on a Malvern Zetasizer Nano-ZS (Malvern, Malvern Hills, UK) in molecular biology grade water in a disposable sizing cuvette for size measurements or clear disposable zeta cuvette for zeta potential measurements.

Kinase activity assay. Recombinant full-length human SRC activity was detected by luminescence using ADP-Glo™ Kinase Assay + SRC Kinase Enzyme System (Promega), according to manufacturer instructions in half-area solid white 96-well plates at a total volume of 40 μ L. The influence of a range of serial dilutions from 25 x 10⁶ NPs, control NPs or free drug on SRC activity (0.154 ng / μ L) were analyzed by luminescence using a GloMax® Multi (Promega) with an integration time of 0.5s and normalized to internal controls.

Cell culture. MDA-MB-231 cells were cultured in DMEM (Gibco), supplemented with 10% (vol / vol) FBS (Gibco), 2mM L-Glutamine (Gibco) in a standard incubator (95% humidity, 5 % CO₂) and subcultured twice per week. Serum-free medium was used for 6 h during incubations with NPs to prevent nanoparticle aggregation.

Uptake efficiency. For flow cytometry assays, 5 x 10⁵ MDA-MB-231 cells were seeded in 24-well plates and stabilized in an incubator for 18 h. Subsequently 3,000, 1,000, 300, 100, 30, 10, 3 or 0 of **9** / cell or **11** / cell were incubated in 500 μ L of serum-free DMEM to evaluate cellular uptake. After 6 h, an equal volume of DMEM containing 2X FBS was added to all wells and cells were allowed to stabilize overnight. After washing with PBS, living cells were trypsinized for 5 min, washed twice with PBS, and collected in 96 well plates with round bottom. Cells were analyzed by flow cytometry with a BD Fortessa X-20 (Becton Dickinson & Co., NJ, USA) equipped with 4 lasers: Blue Laser (488 nm) FSC, Red Laser (640 nm), Violet Laser (405 nm) and a Yellow Green Laser (561 nm) with automated plate loader system BD HTS. The Cy5 emission fluorescence was detected in the APC channel (640-670 / 30 nm). The data were analyzed using BD FACSDiva software version 8.0.1 for data acquisition and FlowJo® (Flowjo, LLC, OR, USA) for data analysis. Gate thresholds were adjusted to non-nanofected cells and **5** nanofected cells and maintained throughout the experiments. Percentages of cells containing **9** or **11** were represented versus log (ratios NP/cell) and adjusted to a sigmoidal dose-response curve using GraphPad Prism Software. MNF50 values were calculated as the ratio NP / cell necessary to obtain a 50 % of cells containing nanoparticles.

Confocal microscopy colocalization. MDA-MB-231 cells were seeded on 10 mm poly-L-Lysine pre-coated coverslips in 24 well plates (10000 cells/well). In parallel, 6 x 10⁷ of **9**, **11**, **5** or NP-free controls were incubated in 10 μ L 5 % BSA / H₂O overnight at 4 °C to block unspecific bind-

ing³⁴ (Supp. Info.). Nanoparticles were thoroughly dispersed in a sonication bath for 15 min. Cells were then incubated in the presence or in the absence of 3000 NPs in 500 μ L of serum-free DMEM in duplicates. After 6 h, 500 μ L of DMEM supplemented with 2x FBS were added to each of the wells and cells were kept in an incubator for other 18 h. NPs and cells were then fixed with paraformaldehyde (4 % v/v) for 10 min and washed 3 times with PBS every 5 min. Cells were permeabilized for 15 min with 0.3 % Tween / PBS and washed 3 times with PBS every 5 min. Coverslips were incubated in blocking buffer (0.3 % BSA, 10 % FBS, 5 % non-fat dry milk, 0.1 % Tween in PBS) for 30 min. Anti-Src Rabbit mAb (Cell Signaling Technology) was incubated in milk-free blocking buffer (0.3 % BSA, 10 % FBS, 0.1 % Tween in PBS) for 2 h at a dilution of 1:400. After washing 3 times in 0.1 % Tween / PBS, coverslips were incubated for 30 min with Goat anti-Rabbit IgG (H+L) secondary antibody, DyLight 405 conjugate (ThermoFisher Scientific) in milk-free blocking buffer (0.3 % BSA, 10 % FBS, 0.1 % Tween in PBS) at a dilution of 1 : 400. Coverslips were washed twice with 0.1 % Tween / PBS, and mounted with Mowiol® (Sigma-Aldrich) on a slide. NPs and SRC localization was imaged using a scanning confocal inverted microscope LSM 710 Axio Observer (Carl Zeiss, Jena, Germany). The images were acquired with a Plan-Apochromat 63x / 1.4 OIL DIC M27 immersion objective and software ZEN 2010 (Carl Zeiss, Jena, Germany). Confocal images of **9**, **11**, **5** or NP-free controls in cell lysates and cells were obtained in a sequential mode using the following settings: 1) a 405-nm diode excitation laser (30 mW) at 2 % power, an emission of in a range of 410 nm to 488 nm with a main beam splitter MBS-405, and a pinhole of 1.0 Airy Unit (0.6 μ m optical section); and 2) a 633 nm HeNe excitation laser (5.0 mW) at 15 % power, an emission wavelength range of 636-742 nm with a MBS-488/543/633, and a pinhole of 1.0 Airy Unit (0.7 μ m optical section). Transmitted images were obtained with a T PMT. Z-stack images were recorded in an average range of 6 μ m, 13 slices and a constant interval of 0.5 μ m, according to NP size, to localize 500 nm nanoparticles throughout the cell volume. Images were processed with Software ZEN 2010 Black Edition (Carl Zeiss, Jena, Germany) to obtain overlap coefficient and Pearson's Correlation Coefficient as co-localization coefficients. Both coefficients, crosshair diagrams and mask images were obtained after calibration according to negative controls and maintained for all the experiments (Supp. Inf.). Unpaired t-test statistical analysis of four independent experiments was performed using Graph Pad Prism 5.0 for Windows GraphPad Software, La Jolla California USA, www.graphpad.com.

ASSOCIATED CONTENT

Full synthetic details, characterization spectra, results of control nanoparticles and resins, complementary biological data, confocal microscopy images. This material is available free of charge via the Internet at <http://pubs.acs.org>.

AUTHOR INFORMATION

Corresponding Authors

* E-mail: Asier.Unciti-Broceta@igmm.ed.ac.uk;
rmsanchez@ugr.es

Present Address

* VivaCell Biotechnology España S.L. Parque Científico Tecnológico de Córdoba (Rabanales 21).
C/ Astrónoma Cecilia Payne, 14014 Córdoba (Spain).

Author Contributions

All authors have given approval to the final version of the manuscript.

ACKNOWLEDGMENT

This project was funded by FP7 co-fund Talentia Postdoc under grant agreement 267226 and CEIBioTic CEI2015-MP-BS48. AUB and AMLP are grateful to the EPSRC (EP/N021134/1) for funding. RSM is grateful to the Marie Curie Career Integration Grants within the 7th European Community Framework Programme (FP7-PEOPLE-2011-CIG-Project Number 294142). JDUB thanks Spanish Ministerio de Economía y Competitividad for a Torres Quevedo fellowship (PTQ-13-06046). ADG acknowledges scholarship from the Spanish Ministry of Education (grant FPU14/02181) and the University of Granada, PhD programme in Biomedicine. We are grateful to Dr B. Rubio Ruiz for her insights in the synthesis of derivative **2**. The authors thank SciToons team (scitoons.com) for preparing the graphical abstract.

ABBREVIATIONS

Alk, alkyne; BSA, bovine serum albumin; CuAAC, Cu(I)-catalyzed azide-alkyne cycloaddition; Cy5, cyanine 5; DAS, dasatinib; Dde, 1-(4,4-dimethyl-2,6-dioxacyclohexylidene) ethyl group; FBS, Foetal bovine serum; FDA, Food and Drug Administration; Fmoc, Fluorenylmethyloxycarbonyl protecting group; NMR, nuclear magnetic resonance; MNF50, multiplicity of nanofection 50; MS, mass spectrometry; NP, nanoparticle; PBS, phosphate buffered saline; PEG, polyethylene glycol; TLC, thin layer chromatography.

REFERENCES

- Lee, J. A.; Uhlik, M. T.; Moxham, C. M.; Tomandl, D.; Sall, D. J. Modern Phenotypic Drug Discovery Is a Viable, Neoclassic Pharma Strategy. *J. Med. Chem.* **2012**, *55* (10), 4527–4538.
- Eder, J.; Sedrani, R.; Wiesmann, C. The Discovery of First-in-Class Drugs: Origins and Evolution. *Nature reviews. Drug discovery.* England August 2014, pp 577–587.
- Warchal, S. J.; Unciti-Broceta, A.; Carragher, N. O. Next-Generation Phenotypic Screening. *Future Med. Chem.* **2016**, *8* (11), 1331–1347.
- Moffat, J. G.; Vincent, F.; Lee, J. A.; Eder, J.; Prunotto, M. Opportunities and Challenges in Phenotypic Drug Discovery: An Industry Perspective. *Nat. Rev. Drug Discov.* **2017**, *16* (8), 531–543.
- Terstappen, G. C.; Schlüpen, C.; Raggiaschi, R.; Gaviraghi, G. Target Deconvolution Strategies in Drug Discovery. *Nat. Rev. Drug Discov.* **2007**, *6* (11), 891–903.
- Rix, U.; Superti-Furga, G. Target Profiling of Small Molecules by Chemical Proteomics. *Nat. Chem. Biol.* **2009**, *5* (9), 616–624.
- Kim, D.-J.; Yi, Y.-W.; Kim, J. H. In Situ Monitoring of Bindings between Dasatinib and Its Target Protein Kinases Using Magnetic Nanoparticles in Live Cells. *J. Am. Chem. Soc.* **2008**, *130* (49), 16466–16467.
- Schenone, M.; Dančík, V.; Wagner, B. K.; Clemons, P. A. Target Identification and Mechanism of Action in Chemical Biology and Drug Discovery. *Nat. Chem. Biol.* **2013**, *9* (4), 232–240.
- Hochhaus, A.; Kantarjian, H. The Development of Dasatinib as a Treatment for Chronic Myeloid Leukemia (CML): From Initial Studies to Application in Newly Diagnosed Patients. *J. Cancer Res. Clin. Oncol.* **2013**, *139* (Cml), 1971–1984.

- (10) Das, J.; Chen, P.; Norris, D.; Padmanabha, R.; Lin, J.; Moquin, R. V.; Shen, Z.; Cook, L. S.; Doweiko, A. M.; Pitt, S.; et al. 2-Aminothiazole as a Novel Kinase Inhibitor Template. Structure-Activity Relationship Studies toward the Discovery of N-(2-Chloro-6-Methylphenyl)-2-[[6-[4-(2-Hydroxyethyl)-1-Piperazinyl]-2-Methyl-4-Pyrimidinyl]amino]-1, 3-Thiazole-5-Carboxamide (Dasatinib). *J. Med. Chem.* **2006**, *49* (23), 6819–6832.
- (11) Getlik, M.; Grutter, C.; Simard, J. R.; Kluter, S.; Rabiller, M.; Rode, H. B.; Robubi, A.; Rauh, D. Hybrid Compound Design to Overcome the Gatekeeper T338M Mutation in cSrc. *J. Med. Chem.* **2009**, *52* (13), 3915–3926.
- (12) Li, N.-S.; Gossai, N. P.; Naumann, J. A.; Gordon, P. M.; Piccirilli, J. A. Efficient Synthetic Approach to Linear Dasatinib–DNA Conjugates by Click Chemistry. *Bioconjug. Chem.* **2016**, *27* (10), 2575–2579.
- (13) Bunnage, M. E.; Chekler, E. L. P.; Jones, L. H. Target Validation Using Chemical Probes. *Nat. Chem. Biol.* **2013**, *9* (4), 195–199.
- (14) Altea-Manzano, P.; Unciti-Broceta, J. D.; Cano-Cortés, V.; Ruiz-Blas, M. P.; Valero-Grinan, T.; Diaz-Mochon, J. J.; Sanchez-Martin, R. Tracking Cell Proliferation Using a Nanotechnology-Based Approach. *Nanomedicine (Lond.)* **2017**, *12* (13), 1591–1605.
- (15) Tsakiridis, A.; Alexander, L. M.; Gennet, N.; Sanchez-Martin, R. M.; Livigni, A.; Li, M.; Bradley, M.; Brickman, J. M. Microsphere-Based Tracing and Molecular Delivery in Embryonic Stem Cells. *Biomaterials* **2009**, *30* (29), 5853–5861.
- (16) Sanchez-Martin, R. M.; Alexander, L.; Muzerelle, M.; Cardenas-Maestre, J. M.; Tsakiridis, A.; Brickman, J. M.; Bradley, M. Microsphere-Mediated Protein Delivery into Cells. *Chembiochem* **2009**, *10*, 1453–1456.
- (17) Cárdenas-Maestre, J. M.; Pérez-López, A. M.; Bradley, M.; Sánchez-Martín, R. M. Microsphere-Based Intracellular Sensing of Caspase-3/7 in Apoptotic Living Cells. *Macromol. Biosci.* **2014**, *14*, 923–928.
- (18) Delgado-Gonzalez, A.; Garcia-Fernandez, E.; Valero, T.; Cano-Cortés, M. V.; Ruedas-Rama, M. J.; Unciti-Broceta, A.; Sanchez-Martin, R. M.; Diaz-Mochon, J. J.; Orte, A. Metallofluorescent Nanoparticles for Multimodal Applications. *ACS Omega* **2018**, *3* (1), 144–153.
- (19) Yusop, R. M.; Unciti-Broceta, A.; Johansson, E. M. V.; Sanchez-Martin, R. M.; Bradley, M. Palladium-Mediated Intracellular Chemistry. *Nat. Chem.* **2011**, *3* (3), 239–243.
- (20) Unciti-Broceta, A.; Johansson, E. M. V.; Yusop, R. M.; Sánchez-Martín, R. M.; Bradley, M. Synthesis of Polystyrene Microspheres and Functionalization with Pd0 Nanoparticles to Perform Bioorthogonal Organometallic Chemistry in Living Cells. *Nat. Protoc.* **2012**, *7* (6), 1207–1218.
- (21) Diaz-Mochon, J. J.; Bialy, L.; Bradley, M. Full Orthogonality between Dde and Fmoc: The Direct Synthesis of PNA--Peptide Conjugates. *Org. Lett.* **2004**, *6* (7), 1127–1129.
- (22) Iwaylo, D.; Katja, J.; Søren, H. Synthesis of Polystyrene-Based Random Copolymers with Balanced Number of Basic or Acidic Functional Groups. *J. Polym. Sci. Part A Polym. Chem.* **2010**, *48* (9), 2044–2052.
- (23) Ghosh, K. K.; Ha, H.-H.; Kang, N.-Y.; Chandran, Y.; Chang, Y.-T. Solid Phase Combinatorial Synthesis of a Xanthone Library Using Click Chemistry and Its Application to an Embryonic Stem Cell Probe. *Chem. Commun. (Camb.)* **2011**, *47* (26), 7488–7490.
- (24) Unciti-Broceta, J. D.; Cano-Cortés, V.; Altea-Manzano, P.; Pernagallo, S.; Díaz-Mochón, J. J.; Sánchez-Martín, R. M. Number of Nanoparticles per Cell through a Spectrophotometric Method - A Key Parameter to Assess Nanoparticle-Based Cellular Assays. *Sci. Rep.* **2015**, *5* (May), 10091.
- (25) Kolb, H. C.; Finn, M. G.; Sharpless, K. B. Click Chemistry: Diverse Chemical Function from a Few Good Reactions. *Angew. Chemie - Int. Ed.* **2001**, *40* (11), 2004–2021.
- (26) Meldal, M.; Tornøe, C. W. Cu-Catalyzed Azide-Alkyne Cycloaddition. *Chem. Rev.* **2008**, *108* (8), 2952–3015.
- (27) Jølcck, R. I.; Berg, R. H.; Andresen, T. L. Solid-Phase Synthesis of PEGylated Lipopeptides Using Click Chemistry. *Bioconjug. Chem.* **2010**, *21* (5), 807–810.
- (28) Zhang, Z.; Fan, E. Solid Phase Synthesis of Peptidotriazoles with Multiple Cycles of Triazole Formation. *Tetrahedron Lett.* **2006**, *47* (5), 665–669.
- (29) Thielbeer, F.; Donaldson, K.; Bradley, M. Zeta Potential Mediated Reaction Monitoring on Nano and Microparticles. *Bioconjug. Chem.* **2011**, *22* (2), 144–150.
- (30) Sanchez-Martin, R.; Cano-Cortés, V.; Marchal, J. A.; Perán, M. In Vitro Nanoparticle-Mediated Intracellular Delivery into Human Adipose-Derived Stem Cells. *Methods Mol. Biol.* **2013**, *1058*, 41–47.
- (31) Fraser, C.; Dawson, J. C.; Dowling, R.; Houston, D. R.; Weiss, J. T.; Munro, A. F.; Muir, M.; Harrington, L.; Webster, S. P.; Frame, M. C.; et al. Rapid Discovery and Structure-Activity Relationships of Pyrazolopyrimidines That Potently Suppress Breast Cancer Cell Growth via SRC Kinase Inhibition with Exceptional Selectivity over ABL Kinase. *J. Med. Chem.* **2016**, *59* (10), 4697–4710.
- (32) Lidke, D. S.; Lidke, K. A. Advances in high-resolution imaging – techniques for three-dimensional imaging of cellular structures. *J. Cell Sci.* **2012**, *125*, 2571–2580.
- (33) Zhang, M.; Li, J.; Xing, G.; He, R.; Li, W.; Song, Y.; Guo, H. Variation in the internalization of differently sized nanoparticles induces different DNA-damaging effects on a macrophage cell line. *Arch. Toxicol.* **2011**, *85*, 1575–1588.
- (34) Fan, D.-H.; Yuan, S.-W.; Shen, Y.-M. Surface Modification with BSA Blocking Based on in Situ Synthesized Gold Nanoparticles in Poly(dimethylsiloxane) Microchip. *Colloids Surfaces B Biointerfaces* **2010**, *75* (2), 608–611.

Insert Table of Contents artwork here

